6-13-1996

Measurement of Elastic Φ Photoproduction at HERA

M. Derrick
Argonne National Laboratory

D. Krakauer
Argonne National Laboratory

S. Magill
Argonne National Laboratory

D. Mikunas
Argonne National Laboratory

B. Musgrave
Argonne National Laboratory

See next page for additional authors

Follow this and additional works at: https://digitalcommons.andrews.edu/pubs

Authors

M. Derrick, D. Krakauer, S. Magill, D. Mikunas, B. Musgrave, J. R. Okrasinski, J. Repond, R. Stanek, R. L. Talaga, H. Zhang, Margarita C. K. Mattingly, G. Bari, M. Basile, L. Bellagamba, D. Boscherini, A. Bruni, G. Bruni, R. Bruni, G. Cara Romeo, G. Castellini, L. Cifarelli, F. Cindolo, A. Contin, M. Corradi, I. Gialas, P. Giusti, G. Iacobucci, G. Laurenti, G. Levi, A. Margotti, and T. Massam

Measurement of Elastic ϕ Photoproduction at HERA

ZEUS Collaboration

Abstract

The production of ϕ mesons in the reaction $e^+ p \to e^+ \phi p$ ($\phi \to K^+ K^-$) at a median Q^2 of 10^{-4} GeV^2 has been studied with the ZEUS detector at HERA. The differential ϕ photoproduction cross section $d\sigma/dt$ has an exponential shape and has been determined in the kinematic range $0.1 < |t| < 0.5$ GeV^2 and $60 < W < 80$ GeV. An integrated cross section of $\sigma_{\gamma p \to \phi p} = 0.96 \pm 0.19^{+0.21}_{-0.18}$ μb has been obtained by extrapolating to $t = 0$. When compared to lower energy data, the results show a weak energy dependence of both $\sigma_{\gamma p \to \phi p}$ and the slope of the t distribution. The ϕ decay angular distributions are consistent with s-channel helicity conservation. From lower energies to HERA energies, the features of ϕ photoproduction are compatible with those of a soft diffractive process.

The ZEUS Collaboration

M. Derrick, D. Krakauer, S. Magill, D. Mikunas, B. Musgrave, J.R. Okrasinski, J. Repond, R. Stanek, R.L. Talaga, H. Zhang
Argonne National Laboratory, Argonne, IL, USA [p]

M.C.K. Mattingly
Andrews University, Berrien Springs, MI, USA

G. Bari, M. Basile, L. Bellagamba, D. Boscherini, A. Bruni, G. Bruni, P. Bruni, G. Cara Romeo, G. Castellini[1], L. Cifarelli[2], F. Cindolo, A. Contin, M. Corradi, I. Gialas, P. Giusti, G. Iacobucci, G. Laurenti, G. Levi, A. Margotti, T. Massam, R. Nania, F. Palmonari, A. Polini, G. Sartorelli, Y. Zamora Garcia[3], A. Zichichi
University and INFN Bologna, Bologna, Italy [f]

A. Bornheim, J. Crittenden, T. Doeker[4], M. Eckert, L. Feld, A. Frey, M. Geerts, M. Grothe, H. Hartmann, K. Heinloth, L. Heinz, E. Hilger, H.-P. Jakob, U.F. Katz, S. Mengel, J. Mollen[5], E. Paul, M. Pfeiffer, Ch. Rembser, D. Schramm, J. Stamm, R. Wedemeyer
Physikalisches Institut der Universität Bonn, Bonn, Germany [c]

S. Campbell-Robson, A. Cassidy, W.N. Cottingham, N. Dyce, B. Foster, S. George, M.E. Hayes, G.P. Heath, H.F. Heath, D. Piccioni, D.G. Roff, R.J. Tapper, R. Yoshida
H.H. Wills Physics Laboratory, University of Bristol, Bristol, U.K. [o]

M. Arneodo[6], R. Ayad, M. Capua, A. Garfagnini, L. Iannotti, M. Schioppa, G. Susinno
Calabria University, Physics Dept.and INFN, Cosenza, Italy [f]

A. Caldwell[7], N. Cartiglia, Z. Jing, W. Liu, J.A. Parsons, S. Ritz[8], F. Sciulli, P.B. Straub, L. Wai[9], S. Yang[10], Q. Zhu
Columbia University, Nevis Labs., Irvington on Hudson, N.Y., USA [q]

P. Borzemski, J. Chwastowski, A. Eskreys, M. Zachara, L. Zawiejski
Inst. of Nuclear Physics, Cracow, Poland [j]

L. Adamczyk, B. Bednarek, K. Jeleń, D. Kisielewska, T. Kowalski, M. Przybycień, E. Rulikowska-Zarębska, L. Suszycki, J. Zając
Faculty of Physics and Nuclear Techniques, Academy of Mining and Metallurgy, Cracow, Poland [j]

A. Kotański
Jagellonian Univ., Dept. of Physics, Cracow, Poland [k]

L.A.T. Bauerdick, U. Behrens, H. Beier, J.K. Bienlein, O. Deppe, K. Desler, G. Drews, M. Flasiński[11], D.J. Gilkinson, C. Glasman, P. Göttlicher, J. Große-Knetter, T. Haas, W. Hain, D. Hasell, H. Heßling, Y. Iga, K.F. Johnson[12], P. Joos, M. Kasemann, R. Klanner, W. Koch, U. Kötz, H. Kowalski, J. Labs, A. Ladage, B. Löhr, M. Löwe, D. Lüke, J. Mainusch[13], O. Mańczak, T. Monteiro[14], J.S.T. Ng, D. Notz, K. Ohrenberg, K. Piotrzkowski, M. Roco, M. Rohde, J. Roldán, U. Schneekloth, W. Schulz, F. Selonke, B. Surrow, T. Voß, D. Westphal, G. Wolf, C. Youngman, W. Zeuner
Deutsches Elektronen-Synchrotron DESY, Hamburg, Germany

H.J. Grabosch, A. Kharchilava[15], S.M. Mari[16], A. Meyer, S. Schlenstedt, N. Wulff
DESY-IfH Zeuthen, Zeuthen, Germany

G. Barbagli, E. Gallo, P. Pelfer
University and INFN, Florence, Italy [f]

G. Maccarrone, S. De Pasquale, L. Votano
INFN, Laboratori Nazionali di Frascati, Frascati, Italy [f]

A. Bamberger, S. Eisenhardt, T. Trefzger, S. Wölfle
Fakultät für Physik der Universität Freiburg i.Br., Freiburg i.Br., Germany [c]

I

J.T. Bromley, N.H. Brook, P.J. Bussey, A.T. Doyle, D.H. Saxon, L.E. Sinclair, M.L. Utley,
A.S. Wilson
Dept. of Physics and Astronomy, University of Glasgow, Glasgow, U.K. [o]

A. Dannemann, U. Holm, D. Horstmann, R. Sinkus, K. Wick
Hamburg University, I. Institute of Exp. Physics, Hamburg, Germany [c]

B.D. Burow[17], L. Hagge[13], E. Lohrmann, J. Milewski, N. Pavel, G. Poelz, W. Schott, F. Zetsche
Hamburg University, II. Institute of Exp. Physics, Hamburg, Germany [c]

T.C. Bacon, N. Brümmer, I. Butterworth, V.L. Harris, G. Howell, B.H.Y. Hung, L. Lamberti[18], K.R. Long,
D.B. Miller, A. Prinias[19], J.K. Sedgbeer, D. Sideris, A.F. Whitfield
Imperial College London, High Energy Nuclear Physics Group, London, U.K. [o]

U. Mallik, M.Z. Wang, S.M. Wang, J.T. Wu
University of Iowa, Physics and Astronomy Dept., Iowa City, USA [p]

P. Cloth, D. Filges
Forschungszentrum Jülich, Institut für Kernphysik, Jülich, Germany

S.H. An, G.H. Cho, B.J. Ko, S.B. Lee, S.W. Nam, H.S. Park, S.K. Park
Korea University, Seoul, Korea [h]

S. Kartik, H.-J. Kim, R.R. McNeil, W. Metcalf, V.K. Nadendla
Louisiana State University, Dept. of Physics and Astronomy, Baton Rouge, LA, USA [p]

F. Barreiro, G. Cases, J.P. Fernandez, R. Graciani, J.M. Hernández, L. Hervás, L. Labarga,
M. Martinez, J. del Peso, J. Puga, J. Terron, J.F. de Trocóniz
Univer. Autónoma Madrid, Depto de Física Teoríca, Madrid, Spain [n]

F. Corriveau, D.S. Hanna, J. Hartmann, L.W. Hung, J.N. Lim, C.G. Matthews[20], P.M. Patel,
M. Riveline, D.G. Stairs, M. St-Laurent, R. Ullmann, G. Zacek
McGill University, Dept. of Physics, Montréal, Québec, Canada [a, b]

T. Tsurugai
Meiji Gakuin University, Faculty of General Education, Yokohama, Japan

V. Bashkirov, B.A. Dolgoshein, A. Stifutkin
Moscow Engineering Physics Institute, Moscow, Russia [l]

G.L. Bashindzhagyan[21], P.F. Ermolov, L.K. Gladilin, Yu.A. Golubkov, V.D. Kobrin, I.A. Korzhavina,
V.A. Kuzmin, O.Yu. Lukina, A.S. Proskuryakov, A.A. Savin, L.M. Shcheglova, A.N. Solomin,
N.P. Zotov
Moscow State University, Institute of Nuclear Physics, Moscow, Russia [m]

M. Botje, F. Chlebana, J. Engelen, M. de Kamps, P. Kooijman, A. Kruse, A. van Sighem, H. Tiecke, W. Verk-
erke, J. Vossebeld, M. Vreeswijk, L. Wiggers, E. de Wolf, R. van Woudenberg[22]
NIKHEF and University of Amsterdam, Netherlands [i]

D. Acosta, B. Bylsma, L.S. Durkin, J. Gilmore, C. Li, T.Y. Ling, P. Nylander, I.H. Park, T.A. Romanowski[23]
Ohio State University, Physics Department, Columbus, Ohio, USA [p]

D.S. Bailey, R.J. Cashmore[24], A.M. Cooper-Sarkar, R.C.E. Devenish, N. Harnew, M. Lancaster, L. Lindemann,
J.D. McFall, C. Nath, V.A. Noyes[19], A. Quadt, J.R. Tickner, H. Uijterwaal,
R. Walczak, D.S. Waters, F.F. Wilson, T. Yip
Department of Physics, University of Oxford, Oxford, U.K. [o]

G. Abbiendi, A. Bertolin, R. Brugnera, R. Carlin, F. Dal Corso, M. De Giorgi, U. Dosselli,
S. Limentani, M. Morandin, M. Posocco, L. Stanco, R. Stroili, C. Voci, F. Zuin
Dipartimento di Fisica dell' Universita and INFN, Padova, Italy [f]

J. Bulmahn, R.G. Feild[25], B.Y. Oh, J.J. Whitmore
Pennsylvania State University, Dept. of Physics, University Park, PA, USA [q]

G. D'Agostini, G. Marini, A. Nigro, E. Tassi
Dipartimento di Fisica, Univ. 'La Sapienza' and INFN, Rome, Italy [f]

J.C. Hart, N.A. McCubbin, T.P. Shah
Rutherford Appleton Laboratory, Chilton, Didcot, Oxon, U.K. [o]

E. Barberis, T. Dubbs, C. Heusch, M. Van Hook, W. Lockman, J.T. Rahn, H.F.-W. Sadrozinski, A. Seiden, D.C. Williams
University of California, Santa Cruz, CA, USA [p]

J. Biltzinger, R.J. Seifert, O. Schwarzer, A.H. Walenta, G. Zech
Fachbereich Physik der Universität-Gesamthochschule Siegen, Germany [c]

H. Abramowicz, G. Briskin, S. Dagan[26], A. Levy[21]
School of Physics,Tel-Aviv University, Tel Aviv, Israel [e]

J.I. Fleck[27], M. Inuzuka, T. Ishii, M. Kuze, S. Mine, M. Nakao, I. Suzuki, K. Tokushuku, K. Umemori, S. Yamada, Y. Yamazaki
Institute for Nuclear Study, University of Tokyo, Tokyo, Japan [g]

M. Chiba, R. Hamatsu, T. Hirose, K. Homma, S. Kitamura[28], T. Matsushita, K. Yamauchi
Tokyo Metropolitan University, Dept. of Physics, Tokyo, Japan [g]

R. Cirio, M. Costa, M.I. Ferrero, S. Maselli, C. Peroni, R. Sacchi, A. Solano, A. Staiano
Universita di Torino, Dipartimento di Fisica Sperimentale and INFN, Torino, Italy [f]

M. Dardo
II Faculty of Sciences, Torino University and INFN - Alessandria, Italy [f]

D.C. Bailey, F. Benard, M. Brkic, G.F. Hartner, K.K. Joo, G.M. Levman, J.F. Martin, R.S. Orr, S. Polenz, C.R. Sampson, D. Simmons, R.J. Teuscher
University of Toronto, Dept. of Physics, Toronto, Ont., Canada [a]

J.M. Butterworth, C.D. Catterall, T.W. Jones, P.B. Kaziewicz, J.B. Lane, R.L. Saunders, J. Shulman, M.R. Sutton
University College London, Physics and Astronomy Dept., London, U.K. [o]

B. Lu, L.W. Mo
Virginia Polytechnic Inst. and State University, Physics Dept., Blacksburg, VA, USA [q]

W. Bogusz, J. Ciborowski, J. Gajewski, G. Grzelak[29], M. Kasprzak, M. Krzyżanowski,
K. Muchorowski[30], R.J. Nowak, J.M. Pawlak, T. Tymieniecka, A.K. Wróblewski, J.A. Zakrzewski, A.F. Żarnecki
Warsaw University, Institute of Experimental Physics, Warsaw, Poland [j]

M. Adamus
Institute for Nuclear Studies, Warsaw, Poland [j]

C. Coldewey, Y. Eisenberg[26], U. Karshon[26], D. Revel[26], D. Zer-Zion
Weizmann Institute, Particle Physics Dept., Rehovot, Israel [d]

W.F. Badgett, J. Breitweg, D. Chapin, R. Cross, S. Dasu, C. Foudas, R.J. Loveless, S. Mattingly, D.D. Reeder, S. Silverstein, W.H. Smith, A. Vaiciulis, M. Wodarczyk
University of Wisconsin, Dept. of Physics, Madison, WI, USA [p]

S. Bhadra, M.L. Cardy, C.-P. Fagerstroem, W.R. Frisken, M. Khakzad, W.N. Murray, W.B. Schmidke
York University, Dept. of Physics, North York, Ont., Canada [a]

1   Introduction

Elastic photoproduction of ϕ mesons, $\gamma p \rightarrow \phi p$, has previously been studied at photon-proton centre-of-mass energies up to $W \approx 17$ GeV in fixed target experiments [1, 2, 3]. At these energies the reaction $\gamma p \rightarrow \phi p$ has the characteristics of a soft diffractive process: a cross section rising weakly with the centre-of-mass energy, a steep forward diffractive peak in the t distribution, where t is the four-momentum transfer squared at the proton vertex, and s-channel helicity conservation.

At the energies of the previous experiments, elastic vector meson photoproduction is well described as a soft diffractive process in the framework of the Regge theory [4] and of the Vector Dominance Model (VDM) [5]. In this approach, this reaction is assumed to proceed at high energy through the exchange of a "soft" pomeron trajectory [6] with an effective intercept of $1+\epsilon = 1.08$ and a slope of $\alpha' = 0.25$ GeV^{-2}. Recent experimental results [7] extend the validity of this approach to the high energies of HERA for elastic ρ^0 photoproduction. This approach also provides predictions [6] for the total photoproduction cross section consistent with the measurements made at HERA [8]. In contrast, the predictions of Regge theory fail to describe the recently measured rapidly rising cross sections at HERA for elastic J/ψ photoproduction [9] and for exclusive ρ^0 production ($\gamma^\star p \rightarrow \rho^0 p$) in deep inelastic scattering (DIS) [10]. The measurements for the latter two processes are consistent with perturbative QCD calculations [11, 12]. In these calculations the scale of the process is given by the virtuality Q^2 of the exchanged photon for exclusive DIS ρ^0 production or depends on the mass of the vector meson for elastic J/ψ photoproduction. Perturbative QCD calculations for the proton structure function F_2 are consistent with the data [13] at HERA energies for a scale as small as $Q^2 = 1.5$ GeV^2. If the scale of elastic vector meson photoproduction is given by the mass of the vector meson, the scale of elastic ϕ photoproduction is between that of elastic ρ^0 and J/ψ photoproduction and between that of elastic ρ^0 photoproduction and exclusive DIS ρ^0 production. It is therefore of interest to measure elastic ϕ photoproduction and to see whether the scale of the process is large enough to cause a deviation from the behavior of a soft diffractive process.

The expectations of Regge theory and VDM may also be confronted by a measurement of elastic ϕ photoproduction at HERA energies. In the additive quark model [14] and VDM, the reaction $\gamma p \rightarrow \phi p$ can proceed only by pomeron exchange [15], and is thus a particularly clean example of a diffractive reaction.

This paper reports a measurement with the ZEUS detector at HERA of high energy production of ϕ mesons in the reaction $e^+ p \rightarrow e^+ \phi p$ using events with $Q^2 < 4$ GeV^2 in which neither the scattered proton nor the scattered positron was observed in the detector. The ϕ was observed, via its decay into $K^+ K^-$, in the kinematic range $60 < W < 80$ GeV and $0.1 < p_T^2 < 0.5$ GeV^2, where p_T is the transverse momentum of the ϕ with respect to the beam axis.

2   Kinematics

Figure 1 shows a schematic diagram for the reaction

$$e^+(k)p(P) \rightarrow e^+(k')\phi(V)p(P'),$$

1

where each quantity in parentheses is the four-momentum of the particle.

The kinematics of the inclusive scattering of unpolarised positrons and protons is described by the positron-proton centre-of-mass energy and any two of the following variables:

- $Q^2 = -q^2 = -(k - k')^2$, the negative of the four-momentum squared of the exchanged photon;

- $y = (q \cdot P)/(k \cdot P)$, the fraction of the positron energy transferred to the hadronic final state in the rest frame of the initial state proton;

- $W^2 = (q + P)^2 = -Q^2 + 2y(k \cdot P) + M_p^2$, the centre-of-mass energy squared of the photon-proton system, where M_p is the proton mass.

For the description of the exclusive reaction $e^+ p \rightarrow e^+ \phi p$ ($\phi \rightarrow K^+ K^-$) the following additional variables are required:

- $t = (P - P')^2$, the four-momentum transfer squared at the proton vertex;

- the angle between the ϕ production plane and the positron scattering plane;

- the polar and azimuthal angles of the decay kaons in the ϕ rest frame.

In the present analysis, events were selected in which the final state positron was scattered at an angle too small to be detected in the main ZEUS calorimeter. Thus the angle between the ϕ production plane and the positron scattering plane was not measured. In such untagged photoproduction events the Q^2 value ranges from the kinematic minimum $Q^2_{min} = M_e^2 y^2/(1 - y) \approx 10^{-9}$ GeV^2, where M_e is the electron mass, to the detector limit $Q^2_{max} \approx 4$ GeV^2, with a median Q^2 of approximately 10^{-4} GeV^2. Because of this small Q^2 value, the photon-proton centre-of-mass energy can be expressed as:

$$W^2 \simeq 2(E_\phi - p_{Z\phi})E_p,$$

where E_p, E_ϕ are the energies of the incoming proton and the produced ϕ meson and $p_{Z\phi}$ [1] is the longitudinal momentum of the ϕ meson. Similarly, the four-momentum transfer squared, t, at the proton vertex for $Q^2 = Q^2_{min}$ is given by:

$$t = (q - V)^2 \simeq -p_T^2 .$$

Non-zero values of Q^2 cause t to differ from $-p_T^2$ by less than Q^2, as described elsewhere [7].

---

[1]Throughout this paper use is made of the standard ZEUS right-handed coordinate system in which the positive Z-axis points in the direction of flight of the protons (referred to as the forward direction) and the X-axis is horizontal, pointing towards the center of HERA. The nominal interaction point is at $X = Y = Z = 0$.

2.1 ϕ photoproduction

The γp cross section is related to the $e^+ p$ cross section by:

$$\frac{d^2\sigma^{ep}}{dy dQ^2} = \frac{\alpha}{2\pi}\frac{1}{Q^2}\left[\left(\frac{1+(1-y)^2}{y} - \frac{2(1-y)}{y}\frac{Q^2_{min}}{Q^2}\right) \ \sigma_T^{\gamma^* p}(W,Q^2)+\right.$$

$$\left.\frac{2(1-y)}{y}\sigma_L^{\gamma^* p}(W,Q^2)\right]$$

where $\sigma_T^{\gamma^* p}$ and $\sigma_L^{\gamma^* p}$ are the γp cross sections for transversely and longitudinally polarized photons, respectively.

Using the VDM predictions [5]:

$$\frac{\sigma_L^{\gamma^* p}(W,Q^2)}{\sigma_T^{\gamma^* p}(W,Q^2)} = \xi\frac{Q^2}{M_\phi^2}$$

$$\sigma_T^{\gamma^* p}(W,Q^2) = \frac{\sigma_T^{\gamma p}(W,0)}{(1+Q^2/M_\phi^2)^2} \equiv \frac{\sigma^{\gamma p}(W)}{(1+Q^2/M_\phi^2)^2}$$

where M_ϕ is the ϕ meson mass, and using $\xi = 1$ [16] yields

$$\frac{d^2\sigma^{ep}}{dy dQ^2} = F(y,Q^2)\sigma^{\gamma p}(W)$$

where the function:

$$F(y,Q^2) = \frac{\alpha}{2\pi}\frac{1}{Q^2}\left[\left(\frac{1+(1-y)^2}{y} - \frac{2(1-y)}{y}(\frac{Q^2_{min}}{Q^2} - \frac{Q^2}{M_\phi^2})\right) \ \frac{1}{(1+Q^2/M_\phi^2)^2}\right]$$

is the effective photon flux.

Assuming no strong W dependence, the γp cross section at the average W measured in the experiment is obtained as the ratio of the corresponding $e^+ p$ cross section, integrated over the y and Q^2 ranges covered by the measurement, and the photon flux factor $F(y,Q^2)$ integrated over the same y and Q^2 ranges.

3   Experimental setup

3.1   HERA

During 1994 HERA operated with a proton beam energy of 820 GeV and a positron beam energy of 27.5 GeV. In the positron and the proton beams 153 colliding bunches were stored together with an additional 17 proton and 15 positron unpaired bunches. These additional bunches were used for background studies. The time between bunch crossings was 96 ns. The typical instantaneous luminosity was $1.5 \cdot 10^{30}$ cm^{-2}s^{-1}.

3.2 The ZEUS detector

A detailed description of the ZEUS detector can be found elsewhere [17]. The main components used in this analysis are outlined below.

Charged particle momenta are reconstructed by the vertex detector (VXD) [18], the central tracking detector (CTD) [19] and the rear tracking detector (RTD) [17]. The VXD and the CTD are cylindrical drift chambers placed in a magnetic field of 1.43 T produced by a thin superconducting coil. The vertex detector surrounds the beam pipe and consists of 120 radial cells, each with 12 sense wires. The CTD surrounds the vertex detector and consists of 72 cylindrical layers, organized in 9 superlayers covering the polar angular region $15^o < \theta < 164^o$. The RTD is a planar drift chamber located at the rear of the CTD covering the polar angular region $162^o < \theta < 170^o$. Using the information from the VXD, the CTD and the RTD for the two-track events of this analysis, the primary event vertex was reconstructed with a resolution of 1.4 cm in Z and 0.2 cm in the transverse plane.

The high resolution uranium-scintillator calorimeter CAL [20] is divided into three parts, the forward calorimeter (FCAL), the barrel calorimeter (BCAL) and the rear calorimeter (RCAL), which cover polar angles from 2.6^o to 36.7^o, 36.7^o to 129.1^o, and 129.1^o to 176.2^o, respectively. Each part consists of towers which are longitudinally subdivided into electromagnetic (EMC) and hadronic (HAC) readout cells. The transverse sizes are typically 5×20 cm^2 for the EMC cells (10×20 cm^2 in RCAL) and 20×20 cm^2 for the HAC cells. From test beam data, energy resolutions with E in GeV of $\sigma_E/E = 0.18/\sqrt{E}$ for electrons and $\sigma_E/E = 0.35/\sqrt{E}$ for hadrons have been obtained.

Proton-gas events occuring upstream of the nominal e^+p interaction point are out of time with respect to the e^+p interactions and may thus be rejected by timing measurement made by the scintillation counter arrays Veto Wall, C5 and SRTD respectively situated along the beam line at $Z = -730$ cm, $Z = -315$ cm and $Z = -150$ cm.

The luminosity is determined [21] from the rate of the Bethe-Heitler process $e^+p \rightarrow e^+\gamma p$ where the photon is measured by the LUMI calorimeter located in the HERA tunnel in the direction of the positron beam.

3.3 Trigger

ZEUS has a three level trigger system. The data used in this analysis were taken with the "untagged vector meson photoproduction trigger" described in this section. The photoproduction events are "untagged" since the scattered positron escapes undetected through the beam pipe hole in the RCAL.

The first level trigger (FLT) required:

- a minimum energy deposit of 464 MeV in the electromagnetic section of the RCAL, excluding the towers immediately surrounding the beam pipe;

- at least one track candidate in the CTD;

4

- less than 1250 MeV deposited in the FCAL towers surrounding the beam pipe.

- the time of any energy deposited in the Veto Wall, the C5 and the SRTD to be consistent with an e^+p interaction and not with a proton-gas event.

The second level trigger (SLT) rejected background events exploiting the excellent time resolution of the calorimeter.

The third level trigger (TLT) used information from the CTD to select events with a reconstructed vertex, at most 4 reconstructed tracks and an invariant mass less than 1.5 GeV for at least one two-track combination assuming that the particles are pions. The rate of the untagged vector meson photoproduction trigger leaving the TLT was about 2 Hz. Because of this high rate the trigger was prescaled. The recorded data collected during 1994 from this trigger correspond to an effective integrated luminosity of 887 ± 31 nb^{-1}.

4   Event selection

The following offline cuts were applied to select the reaction $\gamma p \to \phi(\to K^+K^-)p$:

- exactly two oppositely charged tracks associated with a reconstructed vertex;

- each track within the pseudorapidity[2] range $|\eta| < 2.0$ and with a transverse momentum greater than 150 MeV. These cuts select the high efficiency and well understood region of the tracking detector;

- the Z coordinate of the vertex within ± 30 cm of the nominal interaction point;

- in BCAL and RCAL, not more than 200 MeV in any EMC (HAC) calorimeter cell which is more than 30 cm (50 cm) away from the extrapolated impact position of either of the two tracks. This cut rejects events with additional neutral particles;

- energy deposit in FCAL less than 0.8 GeV. This cut reduces the contamination from diffractive proton dissociation, $\gamma p \to \phi X$.

Since the detector geometry and the trigger limit the observable kinematic range for the reaction $\gamma p \to \phi p$, the selected events were restricted to the region:

$$60 < W < 80 \, \text{GeV}$$

$$0.1 < p_T^2 < 0.5 \, \text{GeV}^2,$$

where the acceptance is well understood and the background contamination due to proton dissociation is relatively small.

---

[2]The pseudorapidity η is defined as $\eta = -\ln[\tan(\frac{\theta}{2})]$.

5 Monte Carlo simulation and acceptance calculation

The acceptance for untagged elastic ϕ photoproduction was calculated by Monte Carlo methods. The reaction $e^+p \rightarrow e^+\phi p$ was simulated using two different event generators. The first one, DIPSI, is based on a model by Ryskin [11]. It describes elastic vector meson production by the exchange of a pomeron which interacts with the quark-antiquark pair into which the incoming virtual photon fluctuates. The second generator, JETPHI, uses a VDM approach and was written in the framework of the JETSET package [22].

Events were generated in the W range from 50 to 90 GeV and the Q^2 range between Q^2_{min} and 4 GeV^2. The ϕ decay angular distributions in both programs were simulated assuming s-channel helicity conservation. To reproduce the p_T^2 distribution of the data, the t dependence was taken to be of the form $e^{-b|t|}$ with $b = 7$ GeV^{-2}. The input vertex distribution was simulated in accordance with that measured using non-diffractive photoproduction events.

The generated events were processed through the ZEUS detector and trigger simulation programs as well as through the analysis chain. The same offline cuts were used for the Monte Carlo events and for the data. The reconstructed W, p_T^2 and decay angular distributions of the Monte Carlo sample agree well with those of the data.

The acceptance as a function of W and p_T^2 is shown in Fig. 2. The acceptance drops at low values of W because the decay kaons enter BCAL, not RCAL, thus providing no trigger. At high W as well as at low p_T values the acceptance decreases because the decay kaons emerge at a large polar angle and are not detected by the CTD.

The acceptance as a function of M_{KK}, the invariant mass of the two decay kaons, is flat in the ϕ mass region.

6 Results

6.1 Extraction of the ϕ signal

After applying all selection cuts, the two particle invariant mass was computed for each event, assuming that the two charged particles are kaons. The invariant mass distribution is shown in Fig. 3. The line is a fit to the function:

$$dN/dM_{KK} = BW(M_{KK}) + BG(M_{KK}),$$

where the functions BW and BG describe the resonance shape and background, respectively. The resonance shape was described by a relativistic p-wave Breit-Wigner function convoluted with a Gaussian. The width of the Breit-Wigner function was fixed at the Particle Data Group value of 4.43 ± 0.06 MeV [23]. The background, mainly due to the reaction $\gamma p \rightarrow \rho^0 p$, was taken to be of the form:

$$BG = \alpha(M_{KK} - 2M_K)^\beta,$$

where M_K is the kaon mass.

The fit yields 566 ± 31 $\phi \rightarrow K^+K^-$ mesons after background subtraction. The ϕ mass obtained from the fit is $M_\phi = 1.020 \pm 0.001$ GeV, with an r.m.s. of the Gaussian of 4 MeV, compatible with the experimental resolution. The value of the free parameter β obtained from the fit is $\beta = 0.97 \pm 0.09$.

6.2 ϕ Events from background reactions

The main source of background to the elastic ϕ reaction is the process $\gamma p \to \phi X$, where the proton diffractively dissociates into a hadronic final state X which is not detected in the main calorimeter. The background was evaluated by comparing the number of ϕ events in the data, without the $E_{FCAL} < 0.8$ GeV cut, to a Monte Carlo simulation using the PYTHIA generator [24] of the diffractive proton dissociation reaction $\gamma p \to \phi X$. The mass spectrum of the diffractive events was simulated according to a $d\sigma/dM_X^2 \propto (1/M_X)^{2.25}$ distribution [25]. The t dependence was parametrized with the form $e^{-b|t|}$ with $b = 4$ GeV^{-2}. The contamination of the elastic ϕ photoproduction sample from proton dissociation[3] was estimated to be $(24 \pm 7(\text{stat}) \pm 6(\text{syst}))\%$ in the p_T^2 range between 0.1 and 0.5 GeV^2. The systematic error was estimated by varying the exponent in the diffractive M_X distribution between 2 and 2.5. Similarly, the uncertainty due to varying the generated t slope in the MC sample from 4 GeV^{-2} to 3 GeV^{-2} has been included in the systematic error.

For each bin in p_T^2, the number of events in the ϕ peak was corrected for the background from the diffractive proton dissociation reaction $\gamma p \to \phi X$. The p_T^2 behaviour of this background was taken from the PYTHIA MC simulation.

The background due to a ϕ meson produced in a beam-gas interaction was estimated from the analysis of events coming from unpaired bunches. The values found are 1% for positron- and $< 1\%$ for proton-gas interactions.

6.3 Elastic ϕ photoproduction cross section

The cross section for the reaction $\gamma p \to \phi p$ is given by

$$\sigma_{\gamma p \to \phi p} = \frac{N_\phi}{L \cdot F \cdot BR}$$

where N_ϕ is the number of acceptance corrected ϕ events, BR is the branching ratio of the ϕ decay into $K^+ K^-$ ($49.1 \pm 0.9\%$) [23], L is the effective integrated luminosity and $F = 0.025$ is the photon flux factor integrated over the phase space determined by the selection cuts.

An exponential fit to the acceptance corrected p_T^2 distribution in the range $0.1 < p_T^2 < 0.5$ GeV^2 gives the slope value of $6.5 \pm 1.0(\text{stat})$ GeV^{-2}.

The acceptance corrected t distribution was reconstructed from the measured p_T^2 spectrum using a bin-by-bin correction, given by the ratio of the generated t and the reconstructed p_T^2 distributions in the MC sample. The acceptance corrected t distribution is shown in Fig. 4a. An exponential fit of the form $d\sigma/d|t| = d\sigma/d|t||_{t=0} \cdot e^{-b|t|}$ in the $|t|$ range between 0.1 and 0.5 GeV^2 yields:

$$b = 7.3 \pm 1.0(\text{stat}) \pm 0.8(\text{syst}) \text{ GeV}^{-2}$$

---

[3]The proton diffractive dissociation contamination in this measurement and in elastic ρ^0 photoproduction [7] of $(11 \pm 1(\text{stat}) \pm 6(\text{syst}))\%$ are compatible, taking into account the different acceptance at low p_T^2 and the different p_T^2 regions of the two measurements.

$$\frac{d\sigma_{\gamma p \to \phi p}}{d|t|}\bigg|_{t=0} = 7.2 \pm 2.1(\text{stat}) \pm 1.8(\text{syst}) \ \mu\text{b}/\text{GeV}^2$$

The systematic error of the slope parameter b includes uncertainties from the acceptance calculation (6%) and the applied cuts (9%). The systematic error for $d\sigma/dt|_{t=0}$ is due to the acceptance calculation (14%), the applied cuts (15%) and a normalization uncertainty due to the calorimeter trigger (12%), the signal fitting procedure (7%) and the luminosity measurement (3.5%).

Fig. 4b shows the value of the slope parameter b measured by this experiment together with the results of lower energy photoproduction experiments [2, 26]. The ZEUS measurement, when compared to the fixed target measurements, shows a weak energy dependence of b, as predicted by Regge theory [4]. The slope parameter for elastic ρ^0 photoproduction [7] is $b_\rho = 9.9 \pm 1.2 \pm 1.4$ GeV^{-2} measured in the range $|t| < 0.5$ GeV^2 using a fit of the form $e^{-b|t|+ct^2}$. In the framework of geometric diffractive models, the slope obtained here for the ϕ meson, compared to that of the ρ^0, indicates that the radius of ϕp interaction is smaller than that of $\rho^0 p$.

6.4 Total elastic ϕ photoproduction cross section

The total elastic cross section was obtained by extrapolating the differential cross section to $t = 0$ assuming a simple exponential t dependence. The resulting value of the cross section is:

$$\sigma_{\gamma p \to \phi p} = 0.96 \pm 0.19(\text{stat})^{+0.21}_{-0.18}(\text{syst}) \ \mu\text{b}$$

integrated over the range $|t| < 0.5$ GeV^2 and at an average W of 70 GeV.

The systematic error includes uncertainties from the acceptance calculation (8%), the applied cuts (8%) and the normalization as described in section 6.3. The uncertainty from the proton dissociation background subtraction made in each bin of the p_T^2 distribution has been included in the statistical error. The uncertainty of the t extrapolation has been estimated by using a fit of the form $e^{-b|t|+ct^2}$ with different values of c. Changing the parameter c from 0 to 3 GeV^{-4} increases the cross section by 10%. The range of the variation for the parameter c was taken in accordance with the results obtained in high energy ρ^0 photoproduction [7]. This uncertainty has been included in the systematic error.

The cross section for the process $\gamma p \to \phi p$ from this analysis is compared in Fig. 5 to results at lower γp centre-of-mass energies [2, 27]. The data show a weak energy dependence of the cross section from 2 GeV to 70 GeV, as predicted by Regge theory [4].

The cross section ratio of elastic ϕ and ρ^0 [7] photoproduction at $W = 70$ GeV is $0.065 \pm 0.013(\text{stat})$. The same ratio measured at $W = 17$ GeV [3] is 0.076 ± 0.010. These results show that there is no significant energy dependence of the ϕ/ρ^0 photoproduction cross section ratio in this W range.

6.5 Total ϕp cross section

Using VDM and the optical theorem the ϕ photoproduction cross section at $t = 0$ can be related to the total ϕp cross section by:

$$\frac{d\sigma_{\gamma p \to \phi p}}{d|t|}\bigg|_{t=0} = \frac{4\pi\alpha}{f_\phi^2} \cdot \frac{1+\eta^2}{16\pi} \cdot (\sigma_{tot}^{\phi p})^2$$

where η is the ratio of the real to the imaginary part of the forward ϕp elastic scattering amplitude, $f_\phi^2/4\pi$ is the $\gamma\phi$ coupling constant and α is the fine structure constant. For pure pomeron exchange $\eta = 0$. Taking $f_\phi^2/4\pi = 18.4$ (see e.g. [1], p. 393) yields:

$$\sigma_{tot}^{\phi p} = 19 \pm 7 \text{ mb.}$$

Using a parametrisation [6] based on Regge theory, this result is in agreement with the additive quark model which predicts (see e.g. [28]) $\sigma_{tot}^{\phi p} \simeq \sigma_{tot}^{K^+ p} + \sigma_{tot}^{K^- n} - \sigma_{tot}^{\pi^+ p} = 19.9$ mb at $W = 70$ GeV. The comparison of $\sigma_{tot}^{\phi p}$ to the total $\rho^0 p$ cross section, $\sigma_{tot}^{\rho^0 p} = 28.0 \pm 1.2(\text{stat}) \pm 2.8(\text{syst})$ mb [7], indicates that the ϕp interaction radius is smaller than that of $\rho^0 p$. This is consistent with the comparison in section 6.3 of the ϕ and ρ^0 slopes.

6.6 Decay angular distributions

The ϕ decay angular distributions can be used to determine elements of the ϕ spin-density matrix [29]. In the s-channel helicity frame the decay angle θ_h is defined as the angle between the K^+ and the direction of the recoil proton in the ϕ centre-of-mass frame, while the azimuthal angle ϕ_h is the angle between the ϕ decay plane and the $\gamma\phi$ plane in the γp centre-of-mass frame.

Since in the present experiment the scattered positron and proton were not detected, the decay angles are determined by approximating the direction of the virtual photon by that of the incoming positron. It has been verified by Monte Carlo calculations that this is a good approximation.

The acceptance corrected ϕ decay angular distributions in the kinematic range $0.1 < p_T^2 < 0.5$ GeV^2 are shown in Fig. 6. They have been fitted with the functions [29]:

$$\frac{1}{N} \cdot \frac{dN}{d\cos\theta_h} = \frac{3}{4}\left[1 - r_{00}^{04} + (3r_{00}^{04} - 1)\cos^2\theta_h\right]$$

$$\frac{1}{N} \cdot \frac{dN}{d\phi_h} = \frac{1}{2\pi}(1 - 2r_{1-1}^{04}\cos 2\phi_h),$$

where r_{00}^{04} and r_{1-1}^{04} are two of the ϕ spin-density matrix elements.

Assuming VDM and s-channel helicity conservation, the r_{00}^{04} spin-density matrix element can be expressed as:

$$r_{00}^{04} = \frac{Q^2}{M_\phi^2} \cdot \frac{\varepsilon}{1 + \varepsilon\frac{Q^2}{M_\phi^2}},$$

9

where ε is the ratio of the longitudinally to the transversely polarised photon fluxes. Assuming the Q^2 dependence given in section 2.1, on average $\varepsilon \simeq 0.998$ and $r_{00}^{04} \simeq 0.03$ in the kinematic region under study. The spin-density matrix element r_{1-1}^{04} is expected to be zero under the assumption of s-channel helicity conservation.

The fitted values obtained from the distributions in Fig. 6 are $r_{00}^{04} = -0.01 \pm 0.04$ and $r_{1-1}^{04} = 0.03 \pm 0.05$, consistent with VDM and s-channel helicity conservation.

7 Summary and Conclusions

The photoproduction of ϕ mesons has been measured with the ZEUS detector at HERA. The cross section is $\sigma_{\gamma p \to \phi p} = 0.96 \pm 0.19^{+0.21}_{-0.18}$ μb at $< W > \ = 70$ GeV and for $|t| < 0.5$ GeV^2. In comparison to lower energy measurements this result is consistent with Regge theory which predicts a weak rise of this cross section with increasing W from the exchange of a soft pomeron.

The differential cross section $d\sigma/dt$, determined in the kinematic range $0.1 < |t| < 0.5$ GeV^2, falls exponentially with the slope value $b = 7.3 \pm 1.0 \pm 0.8$ GeV^{-2}. The comparison with lower energy data is consistent with the logarithmic rise of the t slope with W expected by Regge theory.

The spin-density matrix elements measured from the ϕ decay angular distributions are in argeement with s-channel helicity conservation.

At HERA energies, elastic ϕ photoproduction shows the features typical of a soft diffractive reaction. The Regge theory expectations for elastic vector meson production at HERA energies are thus corroborated at the scale given by elastic ϕ photoproduction.

8 Acknowledgement

References

[1] T.H. Bauer et al., Rev. Mod. Phys. 50 (1978) 261.

[2] J. Busenitz et al., Phys. Rev. D40 (1989) 1.

[3] R.M. Egloff et al., Phys. Rev. Lett. 43 (1979) 657.

[4] P.D.B. Collins, Introduction to Regge Theory and High Energy Physics, Cambridge University Press (1977).

[5] J.J.Sakurai, Ann. Phys. 11 (1960) 1;
J.J Sakurai, Phys. Rev. Lett. 22 (1969) 981.

[6] A. Donnachie and P.V. Landshoff, Phys. Lett. B296 (1992) 227.

[7] ZEUS Collab., M. Derrick et al., Z. Phys. C69 (1995) 39;
H1 Collab., S. Aid et al., DESY 95-251.

[8] H1 Collab., T. Ahmed et al., Phys. Lett. B299 (1993) 374;
ZEUS Collab., M. Derrick et al., Z. Phys. C63 (1994) 391;
H1 Collab., T. Ahmed et al., DESY 95-162.

[9] H1 Collab., S. Aid et al., paper EPS-0468 submitted to the International Europhysics
Conference on High Energy Physics, Brussels, Belgium, July 1995;
ZEUS Collab., M. Derrick et al., Phys. Lett. B350 (1995) 120.

[10] ZEUS Collab., M. Derrick et al., Phys. Lett. B356 (1995) 601.

[11] M.G. Ryskin, Z. Phys. C57 (1993) 89.

[12] S.J. Brodsky et al., Phys. Rev. D50 (1994) 3134.

[13] ZEUS Collab., M. Derrick et al., DESY 95-193, accepted by Z. Phys. C.

[14] E.M. Levin and L.L. Frankfurt, JETP Lett. 2 (1965) 65;
H.J. Lipkin, Phys. Rev. Lett. 16 (1966) 71;
H.J. Lipkin, Phys. Lett. B335 (1994) 500.

[15] P.G.O. Freund, Nuovo Cimento 48A (1967) 541.

[16] N.N. Achasov and V.A. Karnekov, Sov. J. Nucl. Phys. 38 (1983) 736.

[17] The ZEUS Detector, Status Report, DESY (1993).

[18] C. Alvisi et al., Nucl. Inst. Meth. A305 (1991) 30.

[19] N. Harnew et al., Nucl. Inst. Meth. A279 (1989) 290;
B. Foster et al., Nucl. Phys. B, Proc-Suppl. B32 (1993) 181;
B. Foster et al., Nucl. Inst. Meth., A338 (1994) 254.

[20] M. Derrick et al., Nucl. Inst. Meth. A309 (1991) 77;
A. Andresen et. al., Nucl. Inst. Meth. A309 (1991) 101;
A. Bernstein et. al., Nucl. Inst. Meth. A336 (1993) 23.

[21] D. Kisielewska et al., DESY-HERA 85-25 (1985);
J.Andruszków et al., DESY 92-066 (1992).

[22] M. Bengtsson and T. Sjöstrand, Comp. Phys. Comm. 39 (1986) 347;
T. Sjöstrand and M. Bengtsson, Comp. Phys. Comm. 43 (1987) 367.

[23] Particle Data Group, L. Montanet et al., Phys.Rev. D50 (1994) 1173.

[24] T. Sjöstrand, Z. Phys. C42 (1989) 301.

[25] CDF Collab., F. Abe et al., Phys. Rev. D50 (1994) 5535.

[26] R. Erbe et al., Phys. Rev. 175 (1968) 1669;
C. Berger et al., Phys. Lett. B39 (1972) 659;
J. Ballam et al., Phys. Rev. D7 (1973) 3150;
H.J. Besch et al., Nucl. Phys. B70 (1974) 257;
H.J. Behrend et al., Phys. Lett. B56 (1975) 408;
D.P. Barber et al., Phys. Lett. B79 (1978) 150;
D. Aston et al., Nucl. Phys. B172 (1980) 1;
M. Atkinson et al., Z. Phys. C27 (1985) 233.

[27] S.I. Alekhin et al., CERN-HERA 87-01 (1987);
"Total Cross-Sections for Reactions of High Energy Particles" Landolt-Bornstein, New
Series, Vol 12b, editor H. Schopper (1987).

[28] B.T. Feld, Models of Elementary Particles, Blaisdell Publishing Company, London (1969).

[29] K. Schilling, P. Seyboth and G. Wolf, Nucl. Phys. B15 (1970) 397;
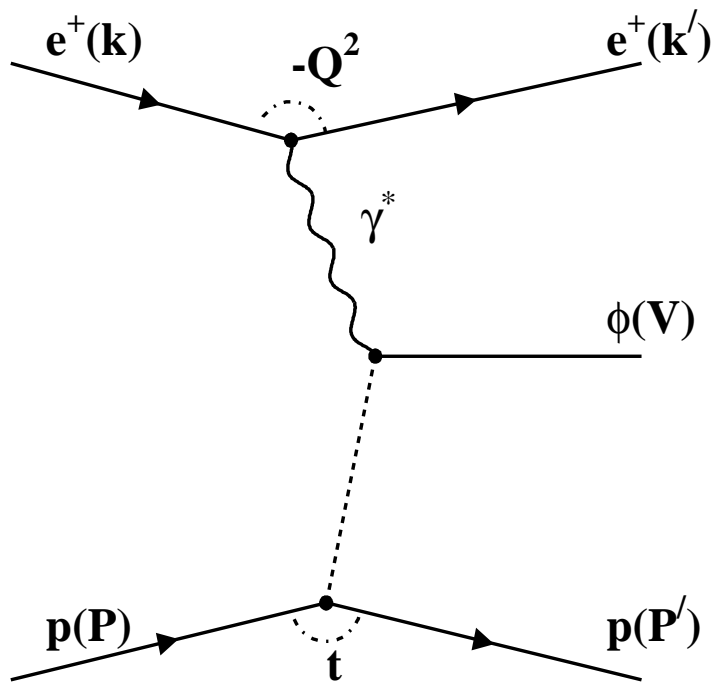K. Schilling and G. Wolf, Nucl. Phys. B61 (1973) 381.

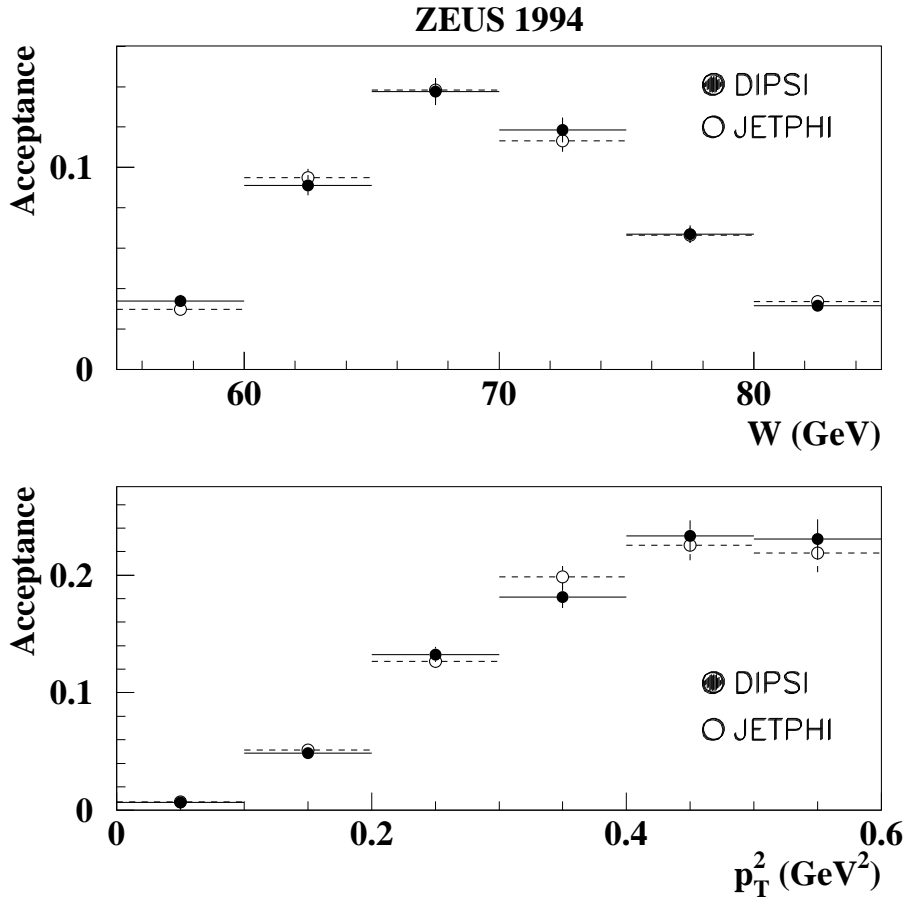Figure 1: Schematic diagram of elastic ϕ photoproduction in e^+p interactions.

Figure 2: Acceptance for the reaction $e^+p \to e^+\phi p$ as a function of W (for $0.1 < p_T^2 < 0.5$ GeV^2) and of p_T^2 (for $60 < W < 80$ GeV) obtained for the two event generators described in the text.
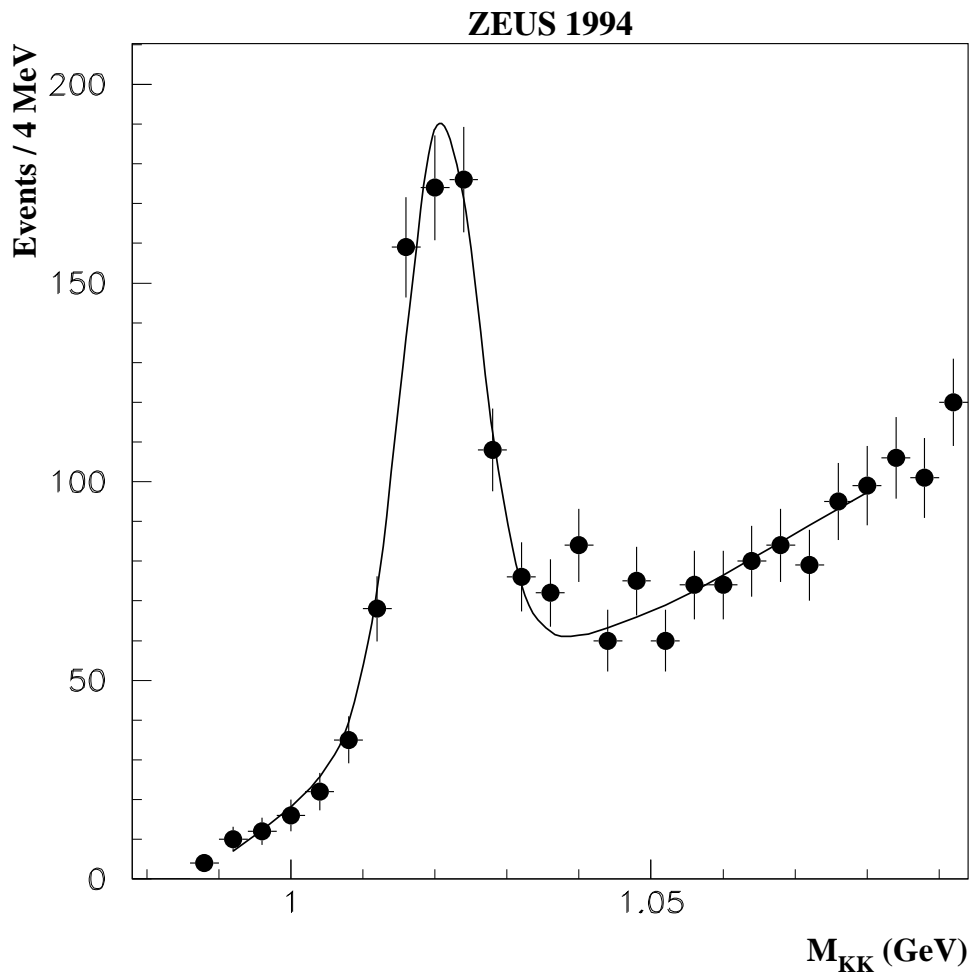
Figure 3: Uncorrected K^+K^- invariant mass distribution for all events passing the final selection cuts. The curve is the result of the fit described in the text.
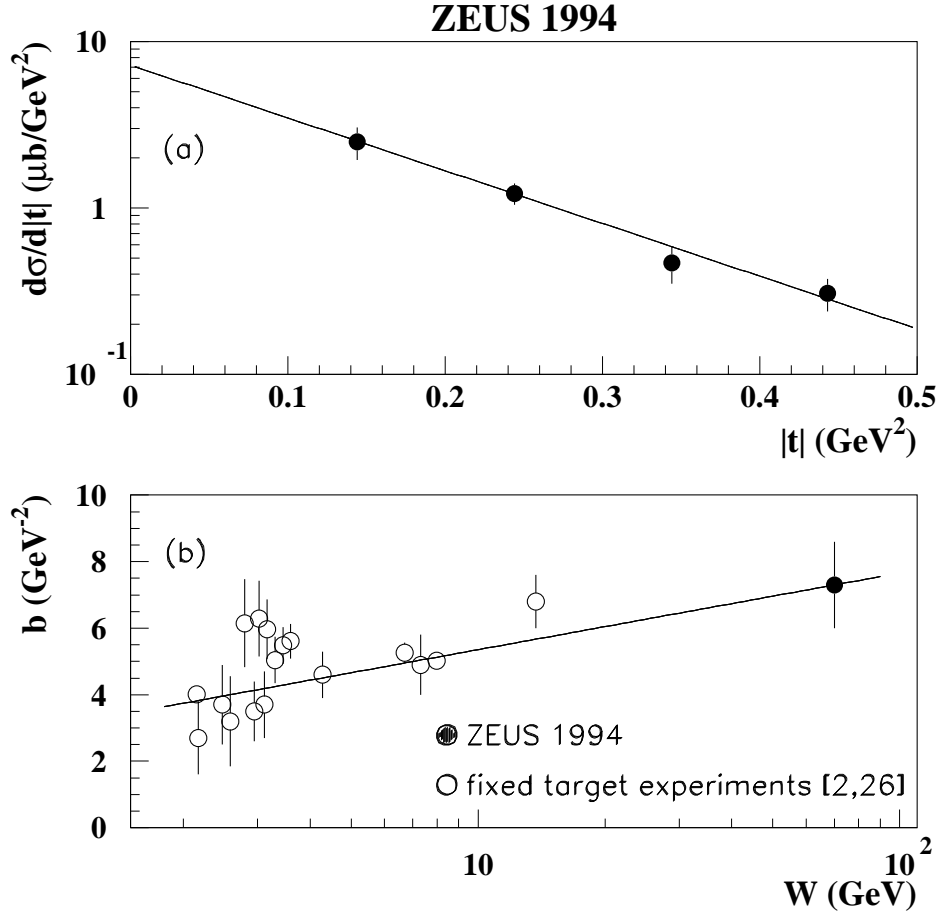
ZEUS 1994

Figure 4: (a) Acceptance corrected t distribution for the reaction $\gamma p \to \phi p$ at $< W > \; = $ 70 GeV. The dots are the ZEUS data, while the line is the result of the exponential fit described in the text. (b) Compilation of measurements of the slope parameter b as a function of W for the reaction $\gamma p \to \phi p$. The different data are measured in various t intervals. The line shows the Regge theory prediction $b_0 + 4\alpha' ln W$ with $\alpha' = 0.25$ GeV^{-2}. The value for b_0 is chosen such that the line intercepts the ZEUS measurement.
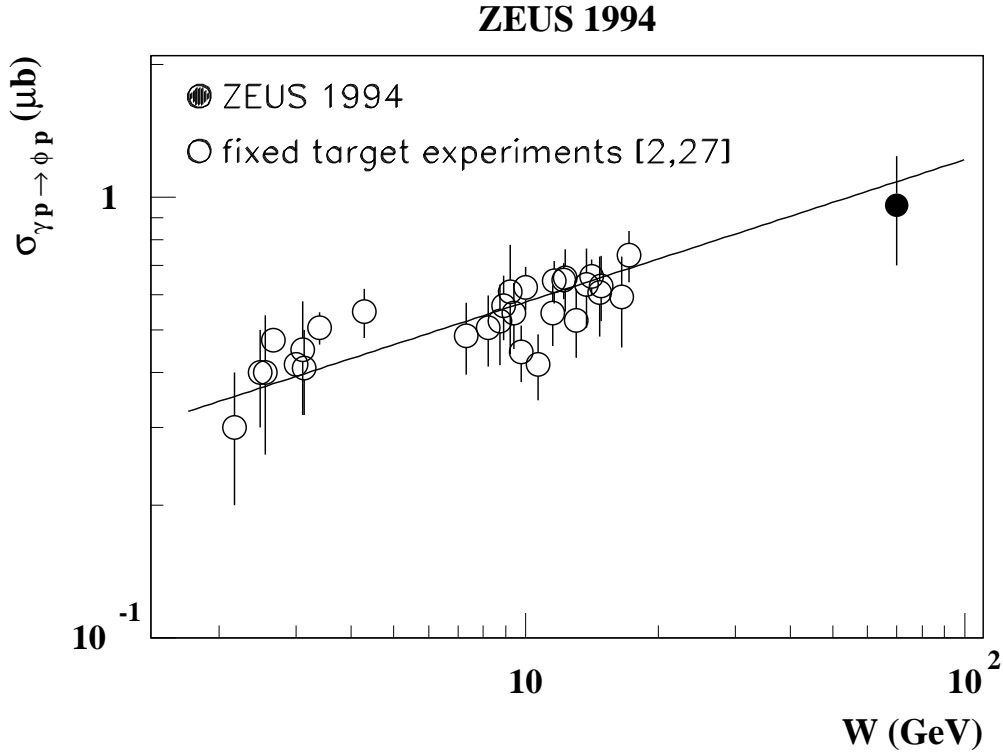
16

ZEUS 1994

Figure 5: Elastic ϕ photoproduction cross sections as a function of W. The solid dot is the ZEUS measurement, while the open circles are the lower energy data. The line shown is a description of the fixed target data using $\sigma_{\gamma p \to \phi p} \propto W^{0.32}$ [6]. It is inspired from Regge theory, which predicts $\sigma_{\gamma p \to \phi p} \propto W^{4\epsilon}/b(W)$, where $1 + \epsilon = 1.08$ is the intercept of the Regge trajectory and $b(W)$ is the energy dependent exponential slope of the differential cross section. This energy dependence however is ignored in the parametrisation.
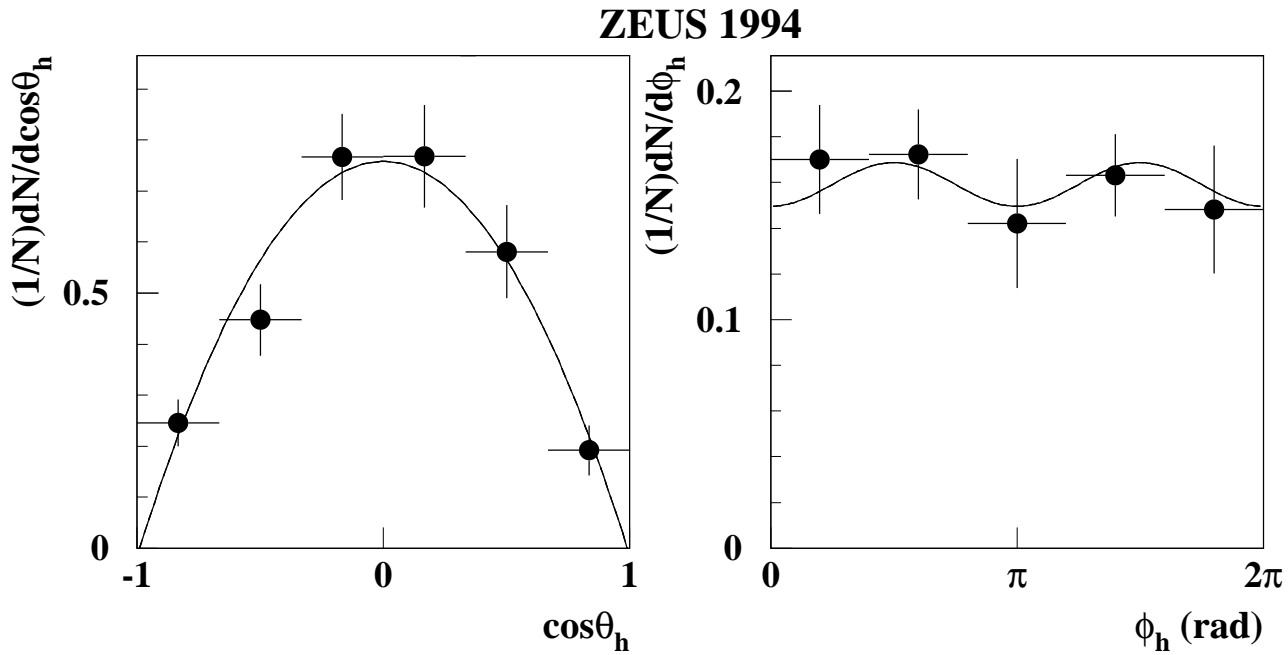
Figure 6: Acceptance corrected decay angular distributions for the ϕ meson in the reaction $\gamma p \to \phi p$ at $< W > = 70$ GeV. The curves are the results of the fits described in the text.